

# ChemComm

Accepted Manuscript



This is an *Accepted Manuscript*, which has been through the Royal Society of Chemistry peer review process and has been accepted for publication.

*Accepted Manuscripts* are published online shortly after acceptance, before technical editing, formatting and proof reading. Using this free service, authors can make their results available to the community, in citable form, before we publish the edited article. We will replace this *Accepted Manuscript* with the edited and formatted *Advance Article* as soon as it is available.

You can find more information about *Accepted Manuscripts* in the [Information for Authors](#).

Please note that technical editing may introduce minor changes to the text and/or graphics, which may alter content. The journal's standard [Terms & Conditions](#) and the [Ethical guidelines](#) still apply. In no event shall the Royal Society of Chemistry be held responsible for any errors or omissions in this *Accepted Manuscript* or any consequences arising from the use of any information it contains.

## All-graphene oxide device with tunable supercapacitor and battery behaviour by the working voltage

Received 00th January 20xx,  
Accepted 00th January 20xx

Chikako Ogata,<sup>\*a</sup> Ruriko Kurogi,<sup>a</sup> Kazuto Hatakeyama,<sup>a</sup> Takaaki Taniguchi,<sup>b</sup> Michio Koinuma<sup>a</sup> and Yasumichi Matsumoto<sup>\*a</sup>

DOI: 10.1039/x0xx00000x

www.rsc.org/

**We propose a new type of all-graphene oxide device. Reduced graphene oxide (rGO)/graphene oxide (GO)/rGO functions as both a supercapacitor and a battery, depending on the working voltage. The rGO/GO/rGO operates as a supercapacitor until 1.2 V. At greater than 1.5 V, it behaves as a battery using redox reaction.**

The global energy paradigm is rapidly transforming from fossil fuels to sustainable energy resources, including solar, wind and geothermal sources.<sup>1</sup> However, power production from these energy resources is not always coincident with energy demand. Therefore, the development of large-scale energy storage systems that resolve this discrepancy is important. Considerable efforts have been expended on the development of high-performance energy storage devices such as Li-ion batteries (LIBs) and supercapacitors (SCs).<sup>2,3</sup> LIBs can commonly deliver a high energy density (150–200 Wh kg<sup>-1</sup>), but are limited by their low power density (less than 1000 W kg<sup>-1</sup>) and poor cycling lifetime (less than 1000 cycles).<sup>2,4</sup> In contrast, SCs can deliver much higher power density (5–10 kW kg<sup>-1</sup>) and exhibit long cycle stability (exceeding 1 × 10<sup>5</sup> cycles) but suffer from a much lower energy density (less than 10 Wh g<sup>-1</sup>).<sup>5</sup> Accordingly, a new energy storage device with the combined characteristics of high energy and power densities and long cycle life is strongly desired as a solution to bridge the gap between LIBs and SCs.<sup>6</sup> In addition, such energy storage devices should preferably be composed of inexpensive, easily acquired materials and be capable of being fabricated through a relatively simple manufacturing process.

Graphene oxide (GO) has recently attracted extensive attention because it offers a low-cost, scalable and wet-chemical approach to graphene. Furthermore, GO exhibits excellent membrane properties, including high water

permeability,<sup>7</sup> good ion and gas selectivity<sup>8</sup> and high proton conductivity;<sup>9</sup> these properties arise from the presence of various oxygenated functional groups. These advantages have led to the application of GO as a solid electrolyte for SCs<sup>10,11</sup> and batteries (e.g. fuel cells,<sup>12</sup> lead-acid batteries<sup>13</sup> and Li-S batteries<sup>14</sup>). In comparison, reduced GO (rGO), which exhibits high electric conductivity and high specific surface area (SSA), can be used in various electrodes of electrical devices such as LIBs, SCs and hybrid Li-ion capacitors.<sup>2,3,15</sup> Although most GO based devices are fabricated either with GO as the electrolyte or with an rGO electrode, an rGO/GO/rGO hybrid structure, which comprises GO electrolyte separator and rGO electrodes, is attractive because of the potential to develop an all-carbon energy device. Such a research direction has been introduced in the literature; however, only the capacitive behaviours of the rGO/GO/rGO structure have been investigated.<sup>10</sup> Its redox behaviours have not yet been focused on, despite the promising applications in energy storage devices.

In this study, we demonstrate a new type of rGO/GO/rGO device that exhibits both supercapacitor and battery behaviour. This device was easily fabricated via photoirradiation of both surfaces of a GO film in a single step. This work, as a solution to bridge the gap between batteries and SCs, sheds new light on the development of energy storage devices.

Fig. 1 illustrates the fabrication steps of the rGO/GO/rGO device. When both surfaces of a GO film were photoirradiated under ambient conditions, the GO film converted into rGO/GO/rGO in a single step (Fig. S1, ESI<sup>†</sup>). Two-sided rGO,

<sup>a</sup> Graduate School of Science and Technology, Kumamoto University, 2-39-1 Kurokami, Chuo-ku, Kumamoto 860-8555, Japan. E-mail: 124d9201@st.kumamoto-u.ac.jp, yasumi@gpo.kumamoto-u.ac.jp; Tel: +81-96-342-3659; Fax: +81-96-342-3679

<sup>b</sup> International Center for Materials Nanoarchitectonics (WPI-MANA), National Institute for Materials Science (NIMS), 1-1 Namiki, Tsukuba, Ibaraki 305-0044, Japan

<sup>†</sup> Electronic Supplementary Information (ESI) available: Experimental details and characterization. See DOI: 10.1039/c000000x/

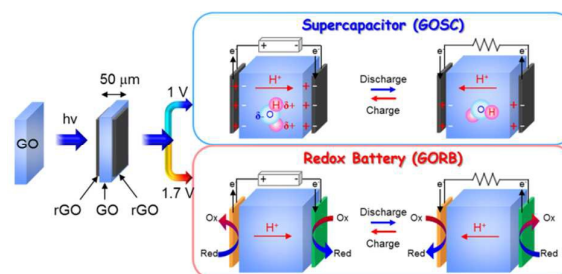


Fig. 1 Schematic of the rGO/GO/rGO device.

which exhibits electrical conductivity, serves as the electrodes. A GO interlayer is retained in the middle and functions as a solid-state electrolyte/separator because of its good ionic conductivity and electronic insulating properties. Moreover, this all-solid-state device is thin (approximately 50  $\mu\text{m}$ ) and completely flexible (Fig. S2, ESI<sup>†</sup>).

To investigate the effect of the photoreduction step, we prepared rGO/GO/rGO using various photoreduction times ranging from 0 to 12 h and tested the electrochemical performance of the resulting devices in the potential window between 0 and 1 V at various scan rates. The cyclic voltammetry (CV) profiles are all rectangular in shape (see Fig. 2a and Figs. S3a–e, ESI<sup>†</sup>), which indicates good double-layer capacitive behaviour. We refer to this device consisting of rGO/GO/rGO as a graphene oxide supercapacitor (GOSC). Compared with other GO-based micro-supercapacitors,<sup>10,18</sup> GOSC exhibited excellent rate performance (Fig. S2f, ESI<sup>†</sup>). This trend confirms that the rGO electrode of GOSC is highly accessible to electrolyte ions such as protons, thus providing high capacitance even when operated at 1,000  $\text{mV s}^{-1}$ . The specific capacitance increases with increasing photoreduction time (Table S1, ESI<sup>†</sup>). GOSC constructed with photo-reduction time of 6 h (GOSC-6 h) exhibits the highest specific areal capacitance of 2  $\text{mF cm}^{-2}$ . The lower capacitance for GOSC-12 h compared to that for GOSC-6 h is attributed to an increase in the electronic conductivity of the GO interlayer.

Because GOSC-6 h exhibited the highest specific capacitance among the fabricated GOSCs, all subsequent electrochemical measurements were carried out on GOSC-6 h. Galvanostatic charge/discharge (CC) curves at different current densities are shown in Fig. 2b and Fig. S4 (ESI<sup>†</sup>). All the curves are nearly isosceles triangles, which indicates high coulombic efficiency and standard double-layer capacitor behaviour. The cyclic stability tests performed on GOSC-6 h are shown in Fig. 2c. After 60 CC cycles at a current density of 0.1 mA, the device retained approximately 80% of its original capacitance. To investigate the cause of capacitance degradation, GOSC-6 h after 100 charge/discharge cycles was analysed by XPS (Fig. S5, ESI<sup>†</sup>). The CH defect of the rGO electrodes converted into C=C and the oxygenated functional groups (particularly, the COC epoxide) of the GO interlayer slightly decreased after 100 charge/discharge cycles. We speculate that the main reasons of capacitance degradation were (1) the decreasing CH defects, which were functioned as active sites of the rGO electrode, and (2) the decreasing electrical insulating property and proton conductivity because of the decreasing oxygenated functional groups of the GO interlayer.

Electrochemical impedance spectroscopy further confirms the superior performance of GOSC (Fig. 2d). The equivalent series resistance obtained from the intercept of the plot on the real axis at high frequency is approximately 80  $\Omega$ , which represents the intrinsic internal resistance of the rGO electrode and the GO electrolyte/separator of GOSC; this resistance reflects the good ionic conductivity of the electrolyte and the low internal resistance of the electrodes. The semicircles at the middle frequency range, which are related to the nature of the interface between GO

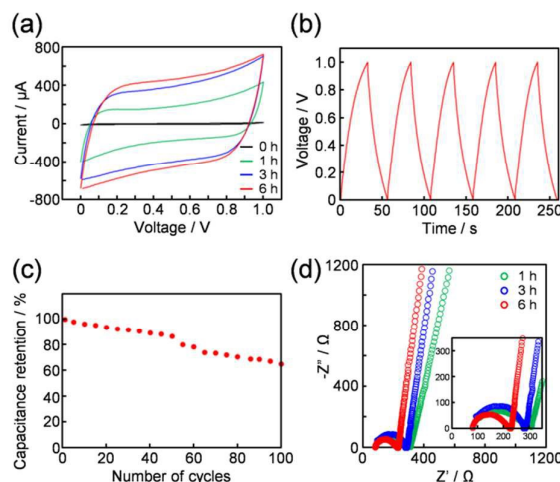


**Fig. 2** (a) CV profiles acquired at a scan rate of 0.3  $\text{V s}^{-1}$  for GOSC prepared using various photoreduction times. (b) CC of GOSC-6 h at 0.1 mA. (c) Performance durability of GOSC-6 h at 0.1 mA. (d) Impedance spectra at various photoreduction times.

electrolyte/separator and the rGO electrode (i.e. charge-transfer resistance), decrease with increasing photoreduction time because of the increasing electronic conductivity of rGO. The X-ray photoelectron spectroscopy (XPS) results and current–voltage ( $I$ – $V$ ) curves confirm this behaviour (Figs. S1 and S6, ESI<sup>†</sup>). Moreover, GOSC exhibits superior frequency response, with an extremely short relaxation time (Fig. S7, ESI<sup>†</sup>). The RC time constant of GOSC-6 h was calculated to be 2.2 sec, in comparison with 10 sec for a commercial activated-carbon supercapacitor.<sup>16</sup> In addition, GOSC-6 h exhibits a small leakage current of 128 nA after 12 h (Fig. S8, ESI<sup>†</sup>). A summary of electrochemical performance of GOSC is provided in Table S1 (ESI<sup>†</sup>). Fig. S10 (ESI<sup>†</sup>) shows a Ragone plot comparing the performance of GOSC obtained by various photoreduction times. It reveals a significant increase in the supercapacitor performance with increasing photoreduction times. Notably, the energy density for GOSC-6 h is calculated to be  $1.1 \times 10^{-4}$   $\text{Wh cm}^{-3}$ , with a power density of 0.12  $\text{W cm}^{-3}$ .

Gao *et al.* fabricated GO-based micro-supercapacitor using a laser technique to write rGO patterns directly on GO films.<sup>10</sup> They reported high specific capacitances of 0.26–0.86  $\text{mF cm}^{-2}$  for their micro-supercapacitors. Notably, although laser treatment results in an increase in the SSA and electrical conductivity of rGO, the capacitance of the GO-based micro-supercapacitor is approximately equal to or less than the 2  $\text{mF cm}^{-2}$  capacitance exhibited by GOSC-6 h.

Given the aforementioned results, surface chemistry rather than SSA is the determining factor for the high capacitive performance of GOSC. In the case of GOSC, the rGO with minimal oxygenated functional groups provides a charged surface area, which strongly affects the wettability of the rGO surfaces accessible to electrolyte ions such as protons. Moreover, we and others have reported that graphite materials with defects such as CH and pentagon–heptagon

pairs can deliver higher capacitance than perfect defect-free graphitic materials.<sup>17</sup> In our case, the XPS spectra showed that the content of COC and C=O groups decreased, whereas that of the C=C groups and CH defects increased after the photoreduction (Fig. S1, ESI<sup>†</sup>). Thus, the rGO structure, which contains minimal oxygenated functional groups and an abundance of defects, is responsible for the devices' high capacitance.

Later, Zhang *et al.* interpreted the capacitive behaviour of GO-based micro-supercapacitor.<sup>18</sup> From molecular dynamic simulations and the anomalous environment of GO interlayers, they proposed a new capacitive model that combines the two distinct charge storage mechanisms of dielectric capacitors and electrochemical capacitors. Therefore, we speculate that the charge storage mechanism of GOSC results from (1) proton conductivity and (2) polarised/separated water molecules in the interlayer spacing of the nanoscale GO.

The fabrication of an all-graphene oxide redox battery (GORB) is a challenge in the field of electronic and energy storage devices. The operation of GO-based devices in a voltage window of *ca.* 2 V has not yet been well developed because the cell voltage of aqueous-electrolyte-based GO devices is usually restricted to 1 V; this narrow voltage window is based on the decomposition voltage of water at 1.23 V.

The rGO/GO/rGO constructed with a photoreduction time of 1 h was measured at potentials higher than 1 V (Figs. 3a and S11, ESI<sup>†</sup>). The CC curves were nearly isosceles triangles until 1.2 V; this shape corresponds to capacitive behaviour, which defines GOSC, as previously discussed. At potentials higher than 1.5 V, a voltage plateau was observed during charge/discharge. Although the plateau potential exhibited an increase in voltage from 1.5 to 2.0 V, the charge voltage of 2.0 V resulted in a large decrease of coulombic efficiency (72% at 1.7 V; 9% at 2.0 V) and discharge time after five cycles (Fig. S11, ESI<sup>†</sup>). This phenomenon indicates that the hydrogen production reaction proceeded during charging at potentials greater than 1.7 V. In addition, the carboxyl group, which is one of the least conductive functional groups and exhibits little reversible redox ability, and CO<sub>2</sub> evolution may result in degradation at 2.0 V.<sup>19</sup> Thus, charge voltages greater than 1.7 V are not suitable for stable operation of GORB.

To understand the effect of photoreduction, we fabricated GORB using various photoreduction times ranging from 0 to 6 h and tested their electrochemical performance in the potential window of 0 to 1.7 V at 0.05 mA (Figs. 3b and S12, ESI<sup>†</sup>). The plateau potential and charge/discharge time increased with increasing photoreduction time. Excellent performance was observed for GORB prepared with a photoreduction time of 3 h (GORB-3 h). Under the hypothesis that the decrease of the charge/discharge time for GORB-6 h is a consequence of its relatively small number of oxygenated functional groups involved in the redox reaction, we conducted further experiments on GORB-3 h.

Figs. 3c, d show typical CV and CC results, respectively, for GORB-3 h. The plateau potential of GORB-3 h observed at approximately 0.75 V corresponds to the difference in the redox potentials for the anode and the cathode. A coulombic

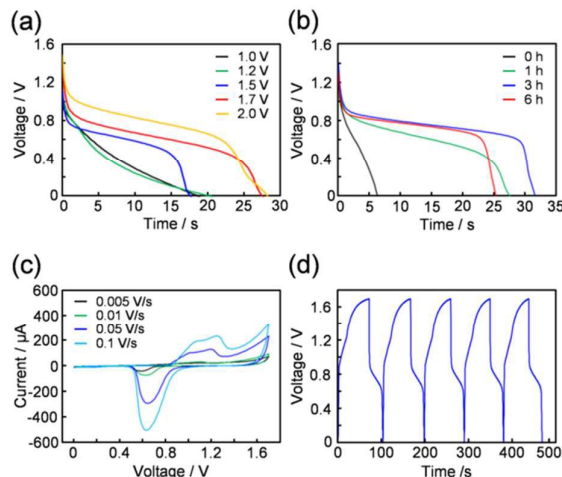


**Fig. 3** (a) Discharge profiles of GORB-1 h charged to various voltages at 0.05 mA. (b) Discharge profiles of GORB prepared with various photoreduction times at 0.05 mA. (c) CV profiles of GORB-3 h at various scan rates. (d) CC of GOSC-3 h at 0.05 mA.

efficiency of approximately 53% was obtained for the charge/discharge cycles of GORB-3 h. Fig. S13 (ESI<sup>†</sup>) shows the cycle stability of GORB-3 h. Approximately 90% of the initial capacitance value of GORB-3 h is maintained after 100 charge/discharge cycles.

Fig. S14 (ESI<sup>†</sup>) shows the XPS spectra for both the anode and the cathode of GORB-3 h after various charge/discharge cycles. The rGO of the cathode was extensively functionalised, whereas far less functionalisation was observed on the rGO anode. This result indicates that the rGO/GO/rGO device, which comprises two different rGO electrodes with redox couples based on two different functional groups with different reaction potentials, functions as a battery. In addition, analysis of the anode of GORB-3 h indicates that CH defects were the main products after 200 charge/discharge cycles. On the other hand, the contents of oxygenated functional groups in the rGO cathode were barely changed.

Recently, Tomai *et al.* demonstrated metal-free aqueous redox capacitors using anthraquinone (AQ: -0.16 V vs. Ag/AgCl) and tetrachlorohydroquinone (TCHQ: 0.50 V vs. Ag/AgCl) supported on nanoporous activated carbon.<sup>20</sup> Moreover, Kobayashi *et al.* demonstrated rechargeable proton exchange membrane fuel-cell batteries fabricated with a modified carbon anode and an RuO<sub>2</sub>/C cathode. They attributed the plateau potential, which appeared at 0.85 V, to the potential difference between the carbonyl/phenol redox reaction on the surface of modified carbon (C-OH ↔ C=O + H<sup>+</sup> + e<sup>-</sup>) and the oxygen evolution reaction (4H<sup>+</sup> + 4e<sup>-</sup> + O<sub>2</sub> ↔ H<sub>2</sub>O).<sup>19</sup>

On the basis of these results, we deduced the following two hypotheses for the redox mechanism of GORB: (1) cathode: C=O + H<sup>+</sup> + e<sup>-</sup> ↔ C-OH; anode: CH (defect) + CO<sub>2</sub> ↔ 2C=O (or C-O) + H<sup>+</sup> + e<sup>-</sup>; or (2) cathode: 4H<sup>+</sup> + 4e<sup>-</sup> + O<sub>2</sub> ↔ H<sub>2</sub>O; anode: CH (defect) + CO<sub>2</sub> ↔ 2C=O (or C-O) + H<sup>+</sup> + e<sup>-</sup>. Researchers have devoted substantial effort to determining

the redox potential of GO.<sup>21</sup> However, to our knowledge, the detailed redox centre and potential of the oxygenated functional groups on GO have not been elucidated. As quinone/hydroquinone molecules have various redox potentials,<sup>22</sup> determining the redox potential of the oxygenated functional groups on GO is inherently difficult. In our case, the oxygenated functional groups on the rGO behave as reactants are not conclusively known. However, as previously mentioned, we assume that the redox couple could be quinone/hydroquinone derived from oxygenated functional groups on the rGO and/or the oxygen evolution reaction. Further investigations are ongoing to obtain more qualitative evidence with respect to how various factors influence the redox performance of GORB.

From a practical viewpoint, the performance of GOSC and GORB should be further improved. Nonetheless, our research demonstrates possibilities of using GOSC/GORB as an advanced energy storage device that can be operated at low temperature and low humidity. We expect that further control and modification of the oxygenated functional groups on GO will enable the fabrication of different types of batteries that operate via various redox reactions. In addition, the nanoscale interlayer of the GO film may serve as unique two-dimensional reaction fields, based on the high water permeability, water polarisation and ionic conductivity, leading to electronic devices that operate on a new mechanism arise.

In conclusion, the rGO/GO/rGO structure functions as both a supercapacitor and a battery under low-humidity and low-temperature conditions, depending on the working voltage. The rGO/GO/rGO structure behaves as a proton-type supercapacitor until 1.2 V. At potentials greater than 1.5 V, this device behaves as a battery operating on the redox reaction between the oxygenated functional groups at the rGO. Finally, the advantages of our proposed device over current energy storage devices are summarised as follows. First, our rGO/GO/rGO device operates without the use of external electrolytes and binders. Second, the simple fabrication process does not require additional processing or complex operations to produce a device that functions as both a supercapacitor and a battery. Third, stacking the device enables an increase in energy density while maintaining the ultrathin construction of the device. These advantages are attractive to develop novel carbon-based energy devices with low fabrication cost and high device performance.

This work was supported by JSPS KAKENHI Grant Number 15J01567.

## Notes and references

- 1 J. A. Turner, *Science*, 1999, **285**, 687-689.
- 2 (a) K. Kang, Y. S. Meng, J. Breger, C. P. Grey, and G. Ceder, *Science*, 2006, **311**, 977-980; (b) F. Bonaccorso, L. Colombo, G. Yu, M. Stoller, V. Tozzini, A. C. Ferrari, R. S. Ruoff, and V. Pellegrini, *Science*, 2015, **347**, 6217.
- 3 (a) M. D. Stoller, S. Park, Y. Zhu, J. An, and R. S. Ruoff, *Nano Lett.*, 2008, **8**, 3498-3502; (b) G. Xiong, C. Meng, R. G. Reifenberger, P. P. Irazoqui, and T. S. Fisher, *Electroanalysis*, 2014, **26**, 30-51.
- 4 B. Dunn, H. Kamath, and J. M. Tarascon, *Science*, 2011, **334**, 928-935.
- 5 (a) Y. Gogotsi and P. Simon, *Science*, 2011, **334**, 917-918; (b) M. F. El-Kady, V. Strong, S. Dubin, and R. B. Kaner, *Science*, 2012, **335**, 1326-1330.
- 6 P. Simon, Y. Gogotsi, and B. Dunn, *Science*, 2014, **343**, 1210-1211.
- 7 R. R. Nair, H. A. Wu, P. N. Jayaram, I. V. Grigorieva, and A. K. Geim, *Science*, 2012, **335**, 442-444.
- 8 (a) H. W. Kim, H. W. Yoon, S. M. Yoon, B. M. Yoo, B. K. Ahn, Y. H. Cho, H. J. Shin, H. Yang, U. Paik, S. Kwon, J. Y. Choi, and H. B. Park, *Science*, 2013, **342**, 91-95; (b) P. Sun, F. Zheng, M. Zhu, Z. Song, K. Wang, M. Zhong, D. Wu, R. B. Little, Z. Xu, and H. Zhu, *ACS Nano*, 2014, **8**, 850-859.
- 9 (a) M. R. Karim, K. Hatakeyama, T. Matsui, H. Takehira, T. Taniguchi, M. Koinuma, Y. Matsumoto, T. Akutagawa, T. Nakamura, S. Noro, T. Yamada, H. Kitagawa, and S. Hayami, *J. Am. Chem. Soc.*, 2013, **135**, 8097-8100; (b) K. Hatakeyama, M. R. Karim, C. Ogata, H. Tateishi, A. Funatsu, T. Taniguchi, M. Koinuma, S. Hayami, and Y. Matsumoto, *Angew. Chem. Int. Ed.*, 2014, **53**, 6997-7000.
- 10 W. Gao, N. Singh, L. Song, Z. Liu, A. L. M. Reddy, L. Ci, R. Vajtai, Q. Zhang, B. Wei, and P. M. Ajayan, *Nat. Nanotechnol.*, 2011, **6**, 496-500.
- 11 (a) X. Yang, F. Zhang, L. Zhang, T. Zhang, Y. Huang, and Y. Chen, *Adv. Funct. Mater.*, 2013, **23**, 3353-3360; (b) X. Yang, L. Zhang, F. Zhang, T. Zhang, Y. Huang, and Y. Chen, *Carbon*, 2014, **72**, 381-386.
- 12 (a) Ravikumar and K. Scott, *Chem. Commun.*, 2012, **48**, 5584-5586; (b) H. Tateishi, K. Hatakeyama, C. Ogata, K. Gezuhara, J. Kuroda, A. Funatsu, M. Koinuma, T. Taniguchi, S. Hayami, and Y. Matsumoto, *J. Electrochem. Soc.*, 2013, **160**, F1175-F1178.
- 13 H. Tateishi, T. Koga, K. Hatakeyama, A. Funatsu, M. Koinuma, T. Taniguchi, and Y. Matsumoto, *ECS Electrochem. Lett.*, 2014, **3**, A19-A21.
- 14 J. Q. Huang, T. Z. Zhuang, Q. Zhang, H. J. Peng, C. M. Chen, and F. Wei, *ACS Nano*, 2015, **9**, 3002-3011.
- 15 H. Kim, K. Y. Park, J. Hong, and K. Kang, *Sci. Rep.*, 2014, **4**, 5278.
- 16 M. F. El-Kady and R. B. Kaner, *Nat. Commun.*, 2013, **4**, 1475.
- 17 (a) H. Tateishi, M. Koinuma, S. Miyamoto, Y. Kamei, K. Hatakeyama, C. Ogata, T. Taniguchi, A. Funatsu, and Y. Matsumoto, *Carbon*, 2014, **76**, 40-45; (b) J. Lin, Z. Peng, Y. Liu, F. Ruiz-Zepeda, R. Ye, E. L. G. Samuel, M. J. Yacaman, B. I. Yakobson, and J. M. Tour, *Nat. Commun.*, 2014, **5**, 5714.
- 18 Q. Zhang, K. Scrafford, M. Li, Z. Cao, Z. Xia, P. M. Ajayan, and B. Wei, *Nano Lett.*, 2014, **14**, 1938-1943.
- 19 K. Kobayashi, M. Nagao, Y. Yamamoto, P. Heo, and T. Hibino, *J. Electrochem. Soc.*, 2015, **162**, F868-F877.
- 20 T. Tomai, S. Mitani, D. Komatsu, Y. Kawaguchi, and I. Honma, *Sci. Rep.*, 2014, **4**, 3591.
- 21 (a) X. Fan, Y. Lu, H. Xu, X. Kong, and J. Wang, *J. Mater. Chem.*, 2011, **21**, 18753-18760; (b) C. M. Chen, Q. Zhang, M. G. Yang, C. H. Huang, Y. G. Yang, and M. Z. Wang, *Carbon*, 2012, **50**, 3572-3584; (c) A. Y. S. Eng, A. Ambrosi, C. K. Chua, F. Sanek, Z. Sofer, and M. Pumera, *Chem. Eur. J.*, 2013, **19**, 12673-12683; (d) G. D. O'Neil, A. W. Weber, R. Buiculescu, N. A. Chaniotakis, and S. P. Kounaves, *Langmuir*, 2014, **30**, 9599-9606; (e) J. Li, C. Chen, J. Wei, J. Li, and X. Wang, *J. Phys. Chem. C*, 2014, **118**, 28440-28447.
- 22 (a) B. Huskinson, M. P. Marshak, C. Suh, S. Er, M. R. Gerhardt, C. J. Galvin, X. Chen, A. Aspuru-Guzik, R. G. Gordon, and M. J. Aziz, *Nature*, 2014, **505**, 195-198; (b) S. Er, C. Suh, M. P. Marshak, and A. Aspuru-Guzik, *Chem. Sci.*, 2015, **6**, 885-893.

Journal Name

## COMMUNICATION

Table of contents (20 words)

Reduced graphene oxide (rGO)/GO/rGO structure operates as a supercapacitor until 1.2 V and as a battery greater than 1.5 V.

